Annual Report for SCEC5 Grant #19039
PI: Toshiro Tanimoto (UCSB) and Robin Matoza (UCSB)
TITLE: "Shallow Elastic Structure from Co-located Seismic and Pressure Sensors"
PERIOD: 2/1/2019 – 1/31/2020

1. Summary

We have developed a new approach to retrieve shallow elastic structure in the upper 50-100 m of the Earth. The method requires a pair of co-located pressure and seismic instruments. By selecting time intervals of large pressure changes, we can quantify elastic response of the Earth to surface pressure changes. Specifically, we measure the quantity $\eta(f) = S_z(f)/S_p(f)$ where f is frequency, S_z is the power spectral density (PSD) of vertical seismic data and S_p is the PSD of surface pressure data. This measurement can be done quite accurately between 0.01 Hz and 0.05 Hz because coherence between pressure and seismic data becomes particularly high in this frequency range. We then invert $\eta(f)$ for elastic parameters at shallow depths using depth sensitivity kernels for which we have developed computer programs.

There were two goals for this one-year grant:
The first goal was to apply this approach to available co-located pressure and seismic data in Southern California and estimate Vs30 at each station. Vs30, an average S-wave speed in the upper 30m of the crust, is an important parameter for ground-motion predictions and is one of the critical parameters for ground-motion prediction equations (e.g., Boore, 1997; Bozorgnia, 2014; Goulet et al., 2017). During the past year, we tested this methodby using co-located nine stations in the Pinyon Flat Observatory. Our estimates agree well with independent estimates by Yong et al. (2016) and an estimate at a borehole site (Fletcher et al., 1990) at nearby stations. We submitted a paper to Geophysical Journal International on these results (Tanimoto and Wang, 2020). We also analzyed co-located seismic and pressure data in Southern California from the period 2000 to 2010. There were 12 such stations and we have analyzed most of them. We have not completed this part of study, however, but expect to finish it in about a month. Also, with a similar method, we analyzed pressure and seismic data from the EarthScope Transportable Array and made our preliminary estimates for all stations.

The second goal was to start a new program to install new infrasound (pressure) sensors at selected existing seismic stations in Southern California to explore the potential utility and logistics of augmenting the Southern California Seismic Network with infrasound sensors. In close collaboration with Dr. Jamie Steidl's group, so far we have installed a new infrasound (pressure) sensor at CPSLO (San Luis Obispo); data are available on IRIS as channels HDF and LDF for station CPSLO network code SB [http://www.iris.washington.edu/mda/SB/CPSLO/]. We are currently working toward adding infrasound capability to station BVDA (Borrego Valley Downhole Array) and GVDA (Garner Valley). We will consider other stations as time and funding permit.

2. Estimates of Vs30 from available co-located pressure and seismic data

(2.1) Basic principles

Since our method for co-located pressure and seismic data is relativelly new, we first describe the underlying processes and explain how it works. For a co-located pressure and seismic data, we first create a pressure-seismic plot like the one in Figure 1 (top-left). This is for an EarthScope station (KMSC) and is not from Southern California but similar features are found at any station. For every 1-hour time interval, over the entire year of 2014, pressure PSD and seismic PSD (3 components) were computed and plotted in Figure 1 (top-left). Vertical seismic data are in blue and horizontal seismic data (sum of PSDs from NS and EW components) are shown in red. In higher pressure ranges, seismic PSDs generally increase. If we compute coherence between pressure and seismic data, coherence is generally quite high for frequncies between 0.01 Hz and 0.05 Hz. Figure 1 is for 0.02 Hz and green points in it are data when coherence was

higher than 0.8. One can see they are found only in a higher pressure range and seismic PSD and pressure PSD have linear relationship.

If we examine phase differences between vertical displacement and pressure for high-coherence time intervals, we get results as shown in three panels at bottom (Figure 1). The bottom-left panel is for KMSC and two other panels are for other stations. Horizontal axes are phase between -180 to 180 degrees and vertical axes are coherence in the three panels. We chose time inetrvals of high pressure (Sp>100 Pa^2/Hz at 0.01 Hz) for these plots. Three panels show that phase differences are about ± 180 degrees when surface pressure is large. This phase relation means that surface pressure and vertical seismic displacements are in the relation as illustrated in the top-right panel of Figure 1. It shows that when pressure waves (related to winds) propagate, ground surface deforms with opposite phase; this is essentially the surface pressure loading on the Earth's surface; when pressure is high, surface is pushed downward and vice versa. We can quantify this elastic response by the ratio $\eta(f) = S_z/S_p$ where f is frequency, S_z is the vertical seismic velocity power spectral density (PSD) and S_p is the pressure PSD. We measure this quantity from the gradients of high-coherence data (green) from various frequencies between 0.01 Hz and 0.05 Hz.

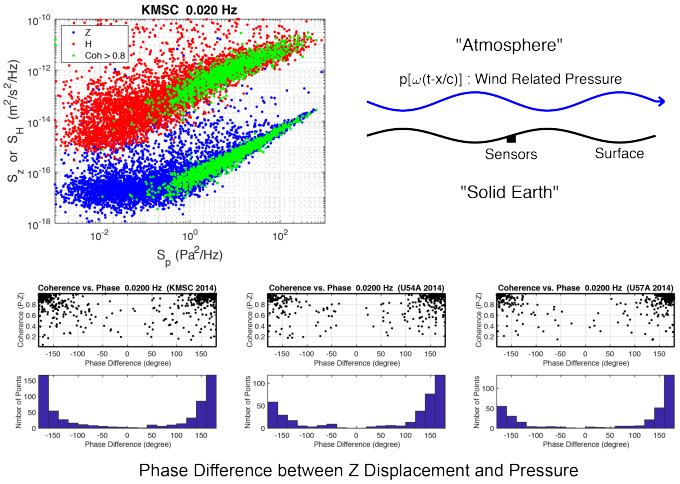

Phase Difference between Z Displacement and Pressure

Figure 1: (top-left) Pressure-seismic plot. Vertical data are in blue and horizontal data are in red. Green points are for the time intervals when coherence between pressure and seismic data are higher than 0.8. For high coherence data, phase difference between vertical displacement and pressure is about 180 degrees as shown at three stations at bottom. These can be interpreted as surface pressure loading effects as illustrated in the top-right figure. When pressure is high, surface is pushed downward and vice versa.

(2.2) Method of Inversion

We have developed theory and wrote a program to compute $\eta(f)$ for a multi-layered medium (Tanimoto and Wang, 2019). In general, $\eta(f)$ should be a function of density (ρ), P-wave velocity (α) and S-wave velocity (β) in the Earth or alternatively it can be expressed as a function of density (ρ), bulk modulus (κ) and rigidity (μ). In the latter case, a formula that connects a perturbation in η and perturbations in ρ, κ, and μ may be written

$$\frac{\delta\eta}{\eta} = \int \{K'_\rho \frac{\delta\rho}{\rho} + K_\kappa \frac{\delta\kappa}{\kappa} + K_\mu \frac{\delta\mu}{\mu}\} dz$$

where K'_ρ, K_κ, and K_μ are depth sensitivity kernels for density, bulk modulus and rigidity. We use this parameterization for the inversion because in this parametrization, we have found that the density kernel becomes almost zero. We can then drop density term and invert data for the rigidity and bulk modulus structures.

We show an example inversion using data from station BPH01. This station is one of the nine stations with co-located sensors in the Pinyon Flat Observatory. We measured $\eta(f)$ between 0.01 Hz and 0.04 Hz

at an interval of 0.005 Hz, which is shown in Figure 2 (left). The starting model (blue) and the inverted models for the first (green dash) and second iterations (red solid) are shown in Figure 2 (right). Since the model did not change beyond the second iteration, we regard the second-iteration model as the final model. The result shows that the data require a low ridigity layer in the upper 20 m of the crust (also low bulk modulus). The difference in rigidity from the deeper range (beyond 20 m) is about 30 percent. The SCEC CVMH model has the surface rigidity about 1.25 GPa which is about the same with rigidity below 20m. This result thus indicates that there is a lower rigidity layer by about 30 percent in the top 20 m.

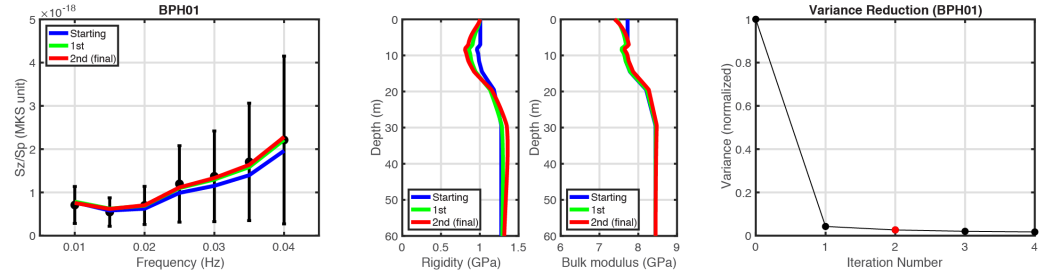

Figure 2: (Left) Measured $\eta(f)$ and the uncertainties (1σ) are shown by black circles and vertical bars. Fit by the starting model (blue), the 1st iteration model (green) and the 2nd iteration model (red). We regard the second-iteration model as the final model. (Middle) Starting model is in blue, the first iteration model in green and the second iteration in red. Both rigidity and bulk modulus models are shown. (Right) Change of variance for each iteration. We continued iteration further, but the fit did not improve after the 2nd iteration.

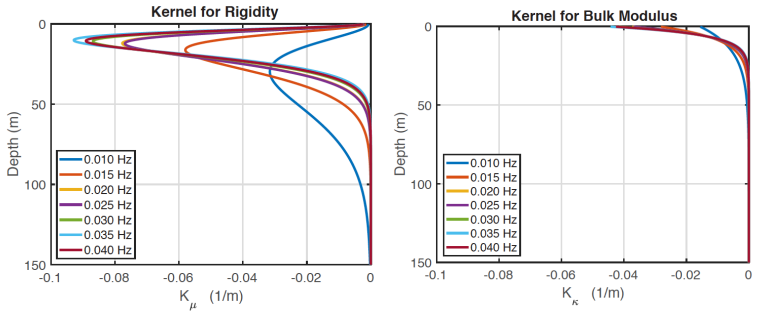

Figure 3: Rigidity kernels (left) and bulk modulus kernels (right) for each frequency (0.10-0.40 Hz).

Figure 3 shows the rigidity kernels (left) and the bulk modulus kernels (right) that were used for the above inversion. Kernel amplitudes indicate that the data are mostly sensitive to rigidity in the upper 100 m for this station with small contribution from bulk modulus near the surface. In the above inversion, we perturbed both parameters but the method mainly constrains the rigidity structure.

(2.3) Vs30 for nine co-located stations in the PFO Array

We applied our inversion method to nine co-located stations in the PFO Array. This array consists of 13 stations from BPH01 to BPH13 but only 9 of them have pressure sensors. We simply use the numbers in the map (Figure 4) to denote a station. For example, 1 in Figure 4 means BPH01, 3 means BPH03 and so forth. Since we invert for rigidity and bulk modulus structures, we need to use empirical relations for density. We used the relationships proposed by Brocher (2005) and Boore (2016) to convert them to S-wave speeds. Then we obtained Vs30 by computing the time-averaged S-wave speed for the upper 30 m of the Earth. The numbers in parentheses in Figure 4 are Vs30 that we estimated. For example, Vs30 at BPH01 is 738 m/s and Vs30 at BPH09 is 975 m/s. Also, in Figure 4, we show an independent estimate by Yong et al. (2016) and another estimate from a borehole structure (Fletcher et al., 1990). Considering the uncertainties associated with the estimates and reported numbers, the agreement between our results and the USGS value (Yong et al., 2016) and the borehole value is quite good. We believe our approach can

provide an independent check for Vs30 estimates and is relatively cost effective as only surface measurements of pressure and seismic data are required.

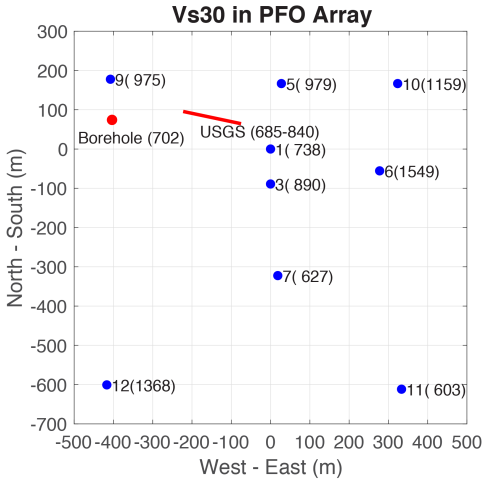

Figure 4: Vs30 estimated by our method for nine stations (blue cirlces). Stations are referenced by numbers; 1 is station BPH01, 3 is BPH03, and so forth. Numbers in the parentheses are our estimates for Vs30 in m/s. There is an independent estimate by Yong et al. (2016) along the red line (685-860 m/s). Red circle is the borehole location (Fletcher et al., 1990). From their S-wave speed structure, we obtained Vs30 of 702 m/s.

(2.4) Vs30 at stations in the EarthScope Transportable Array

Although this effort is for the whole EarthScope Transportable Array and is thus mainly outside Southern California, we supported it partially by this SCEC grant because it helps us understand the nature of our new method. In this study, we obtained the rigidity structures (homogeneous half-space as in Tanimoto and Wang, 2018) and then converted it to Vs30 estimates by using empirical relations. There are distinct large-scale features that are consistent with surface geology data. It also helps us undertsand the differences between the half-space approach and our main layered inversion procedure. A paper was submitted to BSSA.

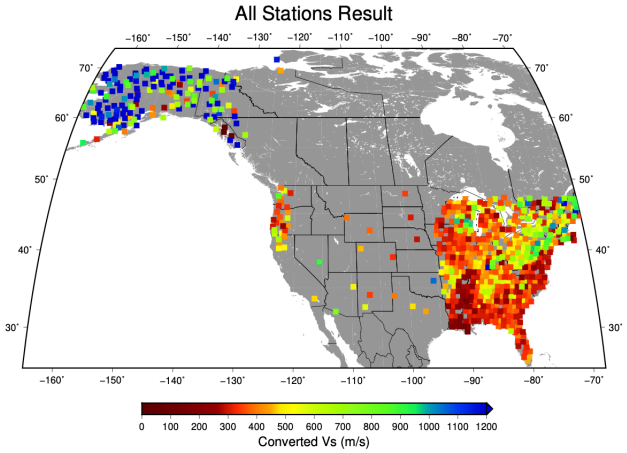

Figure 5: Vs30 for the EarthScope Transportable Array using a simpler, half-space method (Wang and Tanimoto, 2020). Layered inversion approach is still in progress for these data.

3. Pilot Study

Our results demonstrate the potential of augmenting seismic stations with infrasonic pressure sensors for improved ground motion predictions, and we proposed to expand these data collection, analysis, and inversion efforts to a more expansive and spatially dense coverage of the Southern California region. As a pilot program to investigate the utility of expanded infrasound observations (and also evaluate practical logistics), we proposed to operate 2–3 new temporary infrasound stations that will be collocated with existing SCSN stations for approximately 6 months during year 2019.

At the outset of this project, we invested significant time in considering multiple candidate stations balancing logistical considerations with potential scientific returns. We have been collaborating closely with Dr. Jamie Steidl's group on this portion of the project. We are choosing sites primarily on the basis of logistics, with priority given to sites for which details of the local geology are known (e.g., from downhole array, logging, or shallow geophysics). We plan at minimum to install single infrasonic pressure sensors; however, depending upon land and space availability and permiting, we will investigate the potential to install a mini-array of 3 infrasound sensors.

So far, we have installed a new single Hyperion IFS-3111 infrasound (pressure) sensor at CPSLO (San Luis Obispo); data began immediately flowing to IRIS and are available as channels HDF and LDF for station CPSLO network code SB [http://www.iris.washington.edu/mda/SB/CPSLO/]. Initial QC of infrasound data shows microbarom peak is visible and data are of good quality. We expect to analyze these data further after collecting data for about 6 months. CPSLO was an easy initial target given an existing broadband seismometer, accessibility from UC Santa Barbara, and only minor modifications to the seismic vault necessary to install the infrasound sensor. Next in our plan is station BVDA (Borrego Valley Downhole Array); the equipment is prepared and we expect to perform the installation soon. This site represents potential high-value scientific return with the downhole array and knoweldge of near-surface geological structure and site effects. We also plan to install an infrasound sensor at GVDA (Garner Valley) and possibly others as time and funding permit.

We note that our station design is similar to that of the EarthScope TA infrasound sensors. The infrasound sensor is housed in the seismic vault and fitted with a hose attachment. The short hose is connected to the atmosphere through a new port in the vault, which has been engineered to reduce water and insect/rodent intake. For this work, we are utilizing infrasound sensors that belong to PI Matoza's seismo-acoustic laboratory at UC Santa Barbara. These are Hyperion IFS-3111 broadband infrasonic pressure sensors (the sensor type currently used for the EarthScope TA). The availability of this equipment greatly reduces the costs of this proposal and makes the proposed field plans achievable, efficient, and cost-effective. Collaboration with Jamie Steidl and Paul Hegarty has also proven invaluable. In most cases, we are able to use spare channels already available on the digitizer and telemetry systems, greatly reducing the cost and easing logistics for the infrasound installation. Telemetering the data was not part of our original plan but will significantly reduce the number of required site visits. All data collected in this project will be made available at the IRIS DMC.

More generally, recent work has demonstrated the utility of relatively sparse regional seismo-acoustic networks for dramatically enhancing regional and global infrasound signal detection, source location, and discrimination capability [e.g., *Matoza et al.*, 2018]. This project represents a first step toward investigating the utility of a regional seismo-acoustic network in Southern California. Importantly, we are figuring out some of the basic logsitics that would allow for greater expansion of an infrasound network in Southern California should there be interest in future. Graduate students Richard Sanderson, Jiong Wang, and Aaron Anderson (UC Santa Barbara) have gained invaluable field experience and practical knowledge through their involvement with this project.

5. References

Matoza, R.S., D. Fee, D.N. Green, A. Le Pichon, J. Vergoz, M.M. Haney, T.D. Mikesell, L. Franco, O.A. Valderrama, M.R. Kelley, K. McKee, and L. Ceranna (2018), Local, regional, and remote seismo-acoustic observations of the April 2015 VEI 4 eruption of Calbuco volcano, Chile, J. Geophys. Res. Solid Earth, 123, 3814–3827, https://doi.org/10.1002/2017JB015182

Tanimoto, T. and J. Wang (2018), Low-frequency seismic noise characteristics from the analysis of co-located seismic and pressure data, Journal of Geophysical Research: Solid Earth, 123, 2018. https://doi.org/10.1029/2018JB015519

Tanimoto, T. and J. Wang (2019), Theory for deriving shallow elasticity structure from collocated seismic and pressure data, Journal of Geophysical Research: *Solid Earth, 124*, 5811-5835. https://doi.org/10.1029/2018JB017132

Wang, J. and T. Tanimoto (2020), Estimating Near-Surface Rigidity from Low-Frequency Noise using Co-located Pressure and Horizontal Seismic Data, submitted to Bull. Seism. Soc. Am., February, 2020.